Measurement of plasma density using nuclear techniques

J. D. Strachan, R. E. Chrien,[a] and W. W. Heidbrink

Plasma Physics Laboratory, Princeton University, Princeton, New Jersey 08544

(Received 16 August 1982; accepted 29 November 1982)

The magnitude of a fusion reaction rate in a plasma depends strongly on the relative energy of the reacting plasma ions and less strongly on the ion number density. The ratio of two reaction rates, however, is less dependent on the relative velocities while retaining the linear dependence on the relative densities of the plasma ion species. In this manner, the ratio of $t\,(d,n)\alpha$ to $d\,(d,n)\,^3$He fusion reactions depends only on the ratio n_t/n_d, so that tritium levels in a deuterium plasma can be determined from the d–t /d–d reaction ratio ($n_d \simeq n_e$). Similarly, the density of ^{3}He can be determined in a deuterium plasma from the ratio of ^{3}He $(d,p)\alpha$ to $d\,(d,n)\,^3$He fusion reactions. Such measurements of the ^{3}He density are of interest since they relate to the alpha ash removal problem expected on a tokamak reactor.

PACS numbers: 52.70.Nc, 52.55.Gb, 52.55.Pi, 52.25.Lp

I. INTRODUCTION

Determination of the particle transport, edge recycling, and convective heat flow of a plasma all require measurement of the plasma ion density. While the electron density is routinely measured in tokamaks with microwave interferometry and Thomson scattering, the densities of the ionic constituents of a plasma are not easily measured. Possible ion density measurement techniques include mass sensitive charge exchange,[1] which can determine the relative hydrogen and deuterium concentrations, charge exchange enchanced atomic spectroscopy,[2–4] which has determined fully stripped oxygen and carbon concentrations, as well as ordinary atomic spectroscopy, which is useful for determining high Z impurity concentrations.

In this paper, nuclear techniques are reviewed which make use of the $d\,(d,n)\,^3$He, ^{3}He$(d,p)\alpha$, and $t\,(d,n)\alpha$ fusion reactions to measure the densities of deuterium, ^{3}He, and tritium. When these nuclear techniques are applicable they have the advantages of using naturally occurring emissions from the plasma (and are, therefore, nonperturbative), of allowing good time resolution, and of preferentially detecting emissions from the plasma center. Initial applications of these nuclear techniques on the PLT and PDX tokamaks at Princeton include:

(1) Determination of the deuterium density in discharges that follow a switch in the plasma working gas from deuterium to hydrogen. These measurements indicate the fraction of plasma ions contributed by recycled gas and the rate of removal of deuterium from the vacuum vessel.

(2) Determination of the ^{3}He density following short gas puffs of neutral ^{3}He. These measurements indicate the ^{3}He particle transport coefficients from the rise in ^{3}He density following the puff, while the subsequent fall in density provides information on the ^{3}He edge recycling and pumping rates. The rate of removal of ^{3}He from the plasma relates to the alpha ash removal problem in a d–t reactor[5] since ^{3}He and ^{4}He experience similar chemical interactions at the plasma-wall boundary.

(3) Planned determination of the tritium density following laser blow-off injection[6] of trace quantities of tritium. This experiment would be useful for determining tritium transport coefficients as well as for predicting the tritium inventory in d–t machines.

II. METHOD

The total fusion yield in a plasma is

$$I_{12} = \int n_1 n_2 \langle \sigma v \rangle_{12}\, d^3 r, \tag{1}$$

where I is the reaction rate, n_1 is one reactant ion density, n_2 is the other reactant ion density, σ is the fusion cross section, v_{12} is the relative velocity, the integral is over the plasma volume and the average, $\langle\ \rangle$ is over the relative velocities between the 1 and 2 ions. The relative velocities of the reacting ion pairs are determined by the characteristics of the specific plasma and we note that there are two common situations: (a) the plasma ions are Maxwellian so that the fusion reactions are thermonuclear and $\langle \sigma v \rangle$ is a unique function of the plasma ion temperature, or (b) the plasma ions include an energetic ion tail which produces the majority of the fusion reactions, the fusion reactions are no longer thermonuclear and $\langle \sigma v \rangle$ is primarily determined by the characteristics of the energetic ion tail.

The use of Eq. (1) to yield either the particle 1 or 2 density from the measurement of the reaction rate I_{12}, requires accurate knowledge of the relative velocities v_{12} since the fusion reaction cross section is strongly dependent on the relative velocity (Fig. 1). Small uncertainties in the relative velocity lead to large uncertainties in the inferred density. In fact, this was one major difficulty in early studies which determined deuteron densities in plasmas with low magnetic fields using the $d\,(t,n)\alpha$ fusion reaction rate caused by a diagnostic ion beam.[7,8]

An improvement occurs if the ratio of the rates of two reactions is measured. The ratio of the D–^{3}He or d–t fusion rates to the d–d fusion rate can be less sensitive to the relative velocity of the reacting ion pairs than is the individual rate, while retaining the linear dependence on their densities. So far, it has turned out to be useful to create the fusion reactions with a deuterium neutral beam so that the fusion reac-

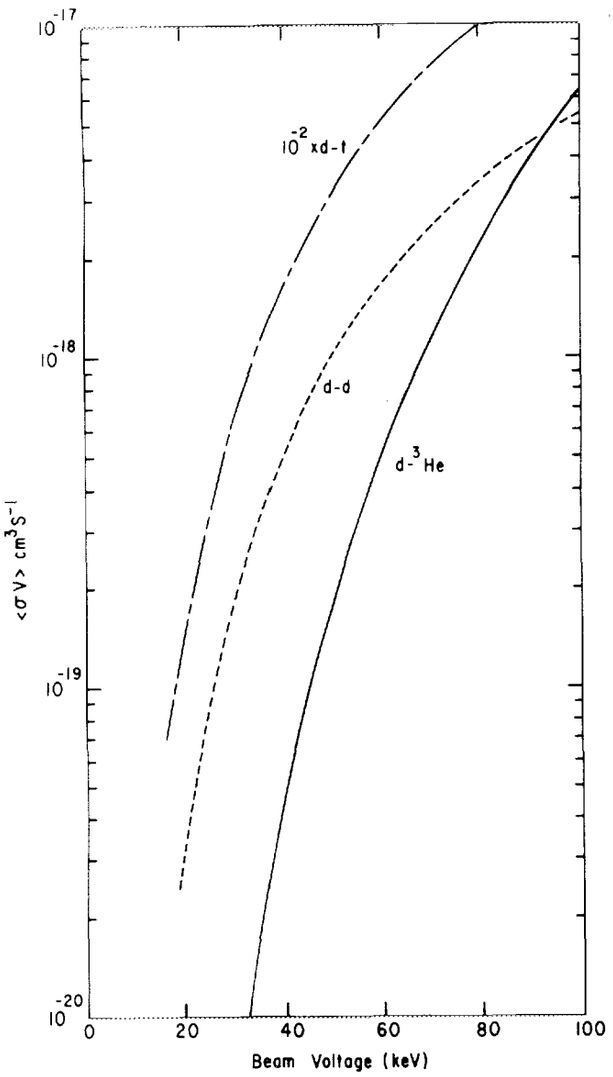

FIG. 1. Reactivities for the $d(d,n)^3$He and ^{3}He$(d,p)\alpha$ fusion reactions as a function of deuteron energy for beam-target reactions.

tions are beam target,[9] and the importance of variations in relative velocity are further reduced since $\langle\sigma v\rangle$ is determined almost entirely by the beam voltage. Creation of the fusion reactions by low power (< 1 MW) neutral beams has the advantages that the injected beam ions have classical slowing down, confinement, and deposition[9] and that the detector count rate is easily chosen by selection of the beam voltage.

For beam-target reactions using a deuterium neutral beam[9]

$$I_{dd} \cong n_d(0)\xi\dot{N}_B\,\tau_{d\text{-}d}\langle\sigma v\rangle_{d\text{-}d},$$
$$I_{d\text{-}^3\mathrm{He}} \cong n_{^3\mathrm{He}}(0)\xi\dot{N}_B\,\tau_{d\text{-}^3\mathrm{He}}\langle\sigma v\rangle_{d\text{-}^3\mathrm{He}},$$
$$I_{dt} \cong n_t(0)\xi\dot{N}_B\tau_{d\text{-}t}\langle\sigma v\rangle_{d\text{-}t}, \qquad (2)$$

where $n_d(0)$, $n_{^3\mathrm{He}}(0)$, and $n_t(0)$ are the central deuterium, ^{3}He, and tritium densities, ξ is the percentage of the full energy component of the neutral beam which is centrally trapped and confined on its first ion orbits; $\dot{N}_B$ is the injection rate of the full energy component ions, $\tau_{d\text{-}d}$, $\tau_{d\text{-}^3\mathrm{He}}$, and $\tau_{d\text{-}t}$ are the cross-section weighted slowing down times of the full energy component ions; and $\langle\sigma v\rangle$ are the respective average cross sections. The ratios

$$R_{d\text{-}^3\mathrm{He}} = I_{d\text{-}^3\mathrm{He}}/I_{d\text{-}d} \propto n_{^3\mathrm{He}}(0)/n_d(0)$$

and

$$R_{d\text{-}t} = I_{d\text{-}t}/I_{d\text{-}d} \propto n_t(0)/n_d(0) \qquad (3)$$

are proportional to the density ratios since the behavior of the deuterium beam is common to all three reactions differing only in the cross-section weighting of the slowing down duration and the relative velocity. Specifically, this means that the beam species mix, neutral beam deposition, beam ion orbit losses on the first orbit, beam power, and beam slowing down rate do not enter into Eq. (3). This would not be true if the beam ions suffered large losses on time scales faster than the cross-section weighted slowing down time or if the slowing down were complex as is possible in tokamaks under some circumstances.

The reduction in sensitivity to the relative velocity is greatest for $R_{d\text{-}t}$. Using the Gammow forms for the cross sections[10]

$$\langle\sigma v\rangle_{dt} = 2.35\times10^{-12}T^{-2/3}\exp(-19.42/T^{1/3})\mathrm{cm}^3/\mathrm{s},$$
$$\langle\sigma v\rangle_{dd} = 3.49\times10^{14}T^{-2/3}\exp(-20.14/T^{1/3})\mathrm{cm}^3/\mathrm{s},$$

we find that

$$R_{dt} = (n_t/n_d)67.3\exp(0.72/T^{1/3}),$$

where T is in units of keV. The ratio $R_{d\text{-}t}$ is plotted in Fig. 1 of Ref. 11 for both beam-target (Fig. 2) and thermonuclear

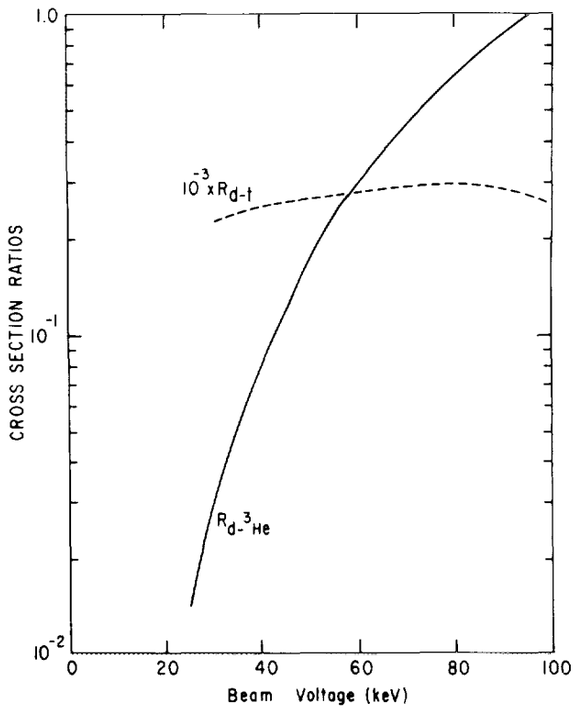

FIG. 2. Ratio of the d–^{3}He to the d–d fusion reaction rates as a function of deuteron energy for beam-target reactions.

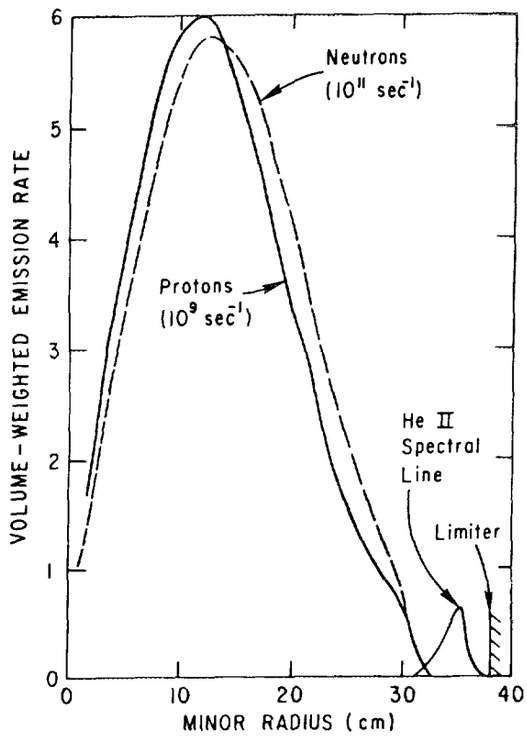

FIG. 3. Radial profiles of the volume averaged d–^{3}He, d–d fusion reaction rates and the ^{3}He II spectral line intensity (all volume-averaged) for the case of PLT neutral beam injection (beam-target fusion reactions).

cases and, as expected from the above, is very insensitive to σv even though each cross section individually is highly sensitive to the relative velocity. In this situation, the strong dependence of the cross section becomes a useful advantage of the technique since the fusion reactions tend to be localized in that part of the plasma containing the most energetic ions (e.g., the plasma center in tokamaks, Fig. 3) which is usually a region of considerable interest.

The ratio technique still retains a strong energy dependence in the determination of the ^{3}He density, however, the ratio $R_{d\text{–}^3\text{He}}$ (Fig. 2) is about 20 times less sensitive to energy in the range 30 to 100 keV than is the d–^{3}He cross section (Fig. 1).

III. EXAMPLES

A. Deuterium density measurement

The application of the ratio technique to the measurement of the deuterium density consists of the comparison of the $d(d,n)$ ^{3}He fusion reaction rates from two discharges in which the relative velocities of the reacting ion pairs are thought to be the same (for example, when the charge exchange ion temperature is measured to be the same). In one of the discharges, the deuteron density is assumed to be given by $n_d \cong n_e$, so that the microwave interferometer yields an approximation to the deuteron density. The deuterium density in the second discharge is then

$$\text{(a)}\ n'_d = n''_e \frac{I'_{dd}}{I''_{dd}}$$

or

$$\text{(b)}\ n'_d = n''_e \left(\frac{I'_{dd}}{I''_{dd}}\right)^{1/2}, \tag{4}$$

depending on (a) if the reactions are of a beam-target nature caused by energetic ions from neutral beam heating or (b) if the reactions are of a thermonuclear nature as caused by the bulk plasma ions. Due to the $n''_d \simeq n''_e$ assumption and the requirement that $\langle\sigma v\rangle' = \langle\sigma v\rangle''$, applications of Eq. (4) tend to have large uncertainties and are, therefore, not too useful. One example in tokamak experiments is when the working gas in the device is changed from deuterium to hydrogen[12,13] then the shot-to-shot decrease in the neutron emission can be used to determine the deuterium concentration. In this situation, the 2.5-MeV neutron emission form $d(d,n)$ ^{3}He can be used to monitor the decrease in deuterium concentration in the plasma or, effectively, the replacement of deuterium with hydrogen in the vessel components. The progression of the deuteron density was measured on a series of PDX diverted discharges (Fig. 4) by the use of the steady-state thermonuclear neutron emission [Eq. 4(b)], by the use of the beam-target neutron emission [Eq. 4(a)] created by a 30-keV diagnostic neutral beam injected at 100 ms, and by the use of the H_2, HD, D_2 peaks in the residual gas analyzer several seconds after the discharge, which is the usual way that such measurements are made.[13] By all three measurements, the deuteron density fell about a factor of 10 after about 30 discharges. The general agreement between the nuclear techniques and the residual gas analyzer indicates that the ratio of hydrogen isotopes in the plasma is similar to the ratio found in the walls[14] and to the molecular concentrations observed several seconds after the discharge.[12] Using the thermonu-

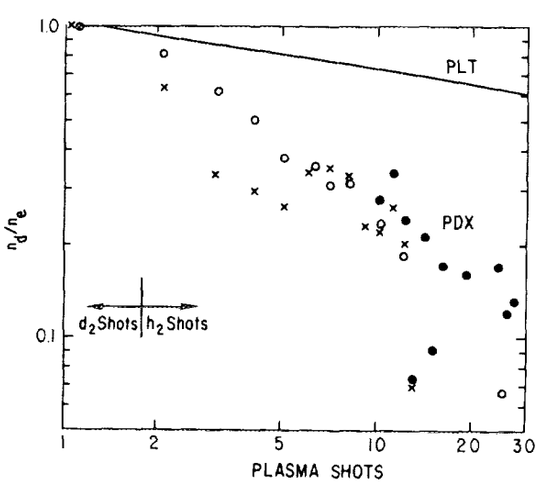

FIG. 4. Deuterium density for a series of PDX discharges where the working gas was changed from deuterium to hydrogen. (×) thermonuclear reactions were used to measure n_d, (●) beam target reactions were used to measure n_d, (○) the residual gas analyzer was used to measure n_d. The line is for a series of discharges on PLT reported in Ref. 12. PDX was operated with its four poloidal diverters for this series of discharges. The PLT vacuum walls had been preloaded with deuterium by glow discharge cleaning. The actual plasma conditions were similar ($B_\phi \sim 25$ kG, $I_\phi \sim 400$ kA, $\bar{n}_e \sim 2\times10^{13}$ cm^{-3}).

clear ratio [Eq. 4(b)] means that one should monitor T_i on each discharge, but in reality such measurements were unavailable in this sequence. This means that 25% changes in T_i that are possible must be considered as an uncertainty in the n_d/n_e determination. For shot 2, one obtains $n_d/n_e \sim 0.3 \rightarrow 2$ which is not too useful, but for shot 30 $n_d/n_e \sim 0.05 \rightarrow 0.2$ has comparable accuracy to the RGA technique. Using the beam-target ratio [Eq. 4(a)] means that one should monitor T_e on each discharge to ensure a constant electron drag, but again such measurements were not available in this sequence. Reasonable expectations for the reproducibility of the plasma T_e and the beam voltage imply that 50% uncertainties in n_d/n_e are obtained. Again, this measurement ability is useful only when n_d/n_e is small.

Clearly, the ^{3}He and tritium density measurements should attain higher reliablility and accuracy since the ratios are measured on the same discharge.

B. Helium density measurements

The application of Eq. (2) to the measurement of ^{3}He densities[15] consists of the comparison of the d–^{3}He reaction rate as measured by the 15-MeV proton emission[16] and the d–d reaction rate as measured by the 2.5-MeV neutron emission. Since there is still a strong relative velocity dependence in the ratio of the cross sections (Fig. 2), ^{3}He density measurements are made with beam-target fusion reactions induced by deuterium neutral beam injection so that the cross section is fixed by the beam voltage. In this case

$$n_{^3\mathrm{He}} \simeq n_d \frac{I_{d\text{-}^3\mathrm{He}}}{I_{d\text{-}d}} \frac{\sigma v_{dd}|_{W_B+3T_i}}{\sigma v_{d\text{-}^3\mathrm{He}^4}|_{W_B+7T_i}} \frac{7}{3}. \tag{5}$$

If we arrange for $n_{^3\mathrm{He}}/n_e$ He small and for n_d/n_e to be a constant, then the central ^{3}He density is

$$n_{^3\mathrm{He}}(t) = C n_e(t) \frac{I_{d\text{-}^3\mathrm{He}}(t)}{I_{dd}(t)} \tag{6}$$

evolution of the ^{3}He density can be obtained without accurate determination of C so long as Z_{eff}, W_B, and T_i remain constant with time. Thus, one useful application of ^{3}He density measurements is when small quantities of ^{3}He are puffed into the edge of a tokamak. As a result of the ^{3}He puff of Fig. 5 the d–^{3}He reaction rate increased by about a factor of 5 while the d–d reaction rate decreased by about 20% (due to increased electron drag on the energetic injected beam ions.)

The principle ^{3}He gas puffing experiments performed to date are on PLT[15] (132 cm major radius, 28 or 38 cm minor radius, 1 $\rightarrow$ 3.2 T toroidal magnetic field, 0.3 $\rightarrow$ 0.6 MA plasma current, 1.0 $\rightarrow$ 5.0$\times 10^{13}$ cm^{-3} line-averaged density, carbon limiters,titanium-gettered vacuum walls) during deuterium neutral beam heating (25 $\rightarrow$ 40 keV beam energy, $\leqslant$1.2 MW beam power, tangential injection.) In these experiments the neutral beam duration was 300 ms. After 100 ms of injection, when the beam-heated plasma was in steady state, ^{3}He gas was puffed for 5 ms (the approximate gas valve exhaust time). The ^{3}He thermalization time is $\lesssim$0.5 ms so we expect the ^{3}He to be in local thermal equilibrium with the plasma deuterons. The quantity of ^{3}He puffed was increased

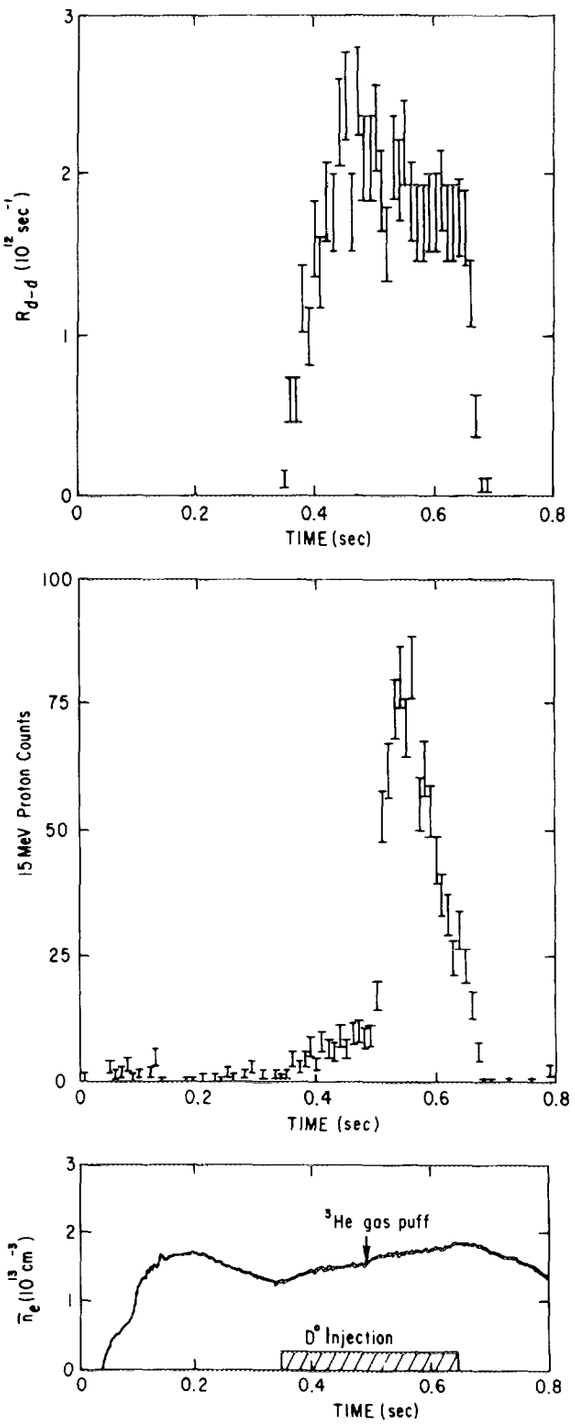

FIG. 5. Time evolution of the d–d reaction rate as measured by the 2.5-MeV neutron emission, the d–^{3}He reaction rate as measured by the 15-MeV proton emission, and the electron density. The reactions are beam-tartet induced by a 35-kV deuterium neutral beam. The 10-ms ^{3}He gas puff caused $\bar{n}_e$ to increase by 10%, the d–^{3}He rate to increase by a factor of 5, and the d–d rate to decrease by 20%.

by increasing the gas puff duration. A direct correlation was observed between the magnitude of the electron density rise associated with the ^{3}He gas puff, the ^{3}He density measured

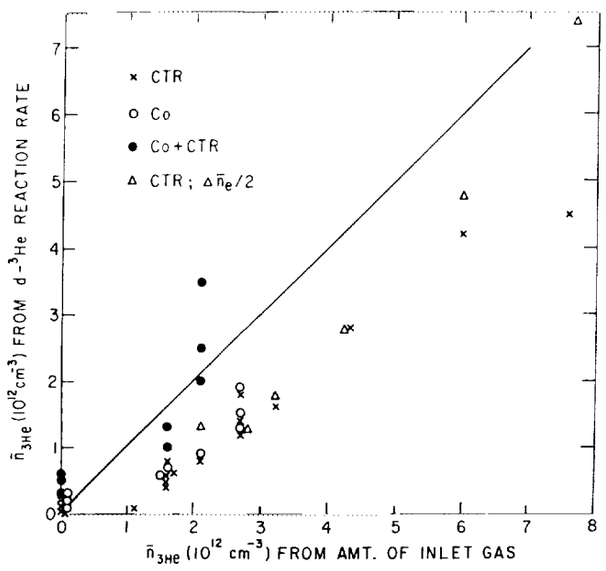

FIG. 6. The line average ^{3}He density rise (nuclear technique) vs the amount of ^{3}He puffed into the PLT vessel. The (Δ) points are one-half the electron density rise resulting from the ^{3}He puff.

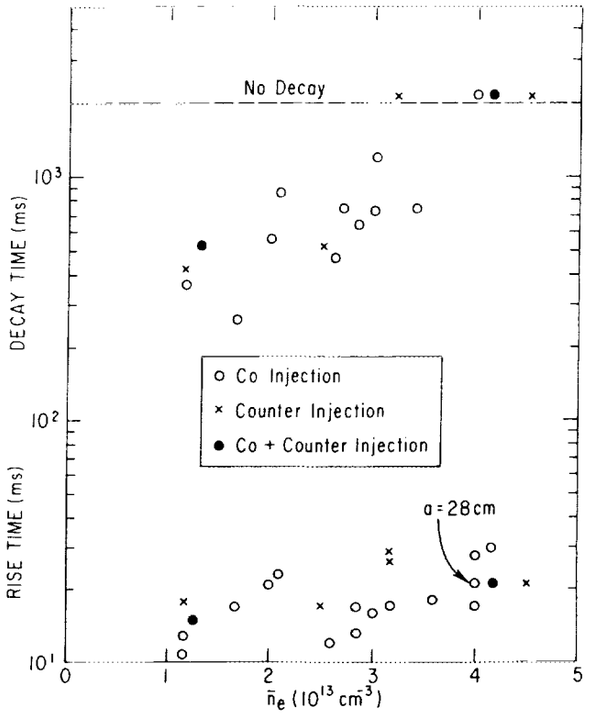

FIG. 8. ^{3}He penetration (τ_R) and exhaust (τ_F) times vs line average density.

by the nuclear technique, and the amount of ^{3}He puffed into the vessel as determined by an ionization gauge (Fig. 6). The main uncertainty in using Eq. (5) to determine the ^{3}He density is the absolute calibration of the 15-MeV proton detector. This calibration consists of determining the percentage of 15-MeV protons that escape the plasma on orbits that strike a surface barrier detector mounted at the vacuum vessel.[17] While the absolute ^{3}He concentration was determined to about a factor of 2 accuracy, the determination of the time evolution of the relative ^{3}He concentration from Eq. (6) is limited only by counting statistics.

The ^{3}He gas puff was accompanied by an increase in the ^{3}He II spectral line [Fig. 7(a)] which was excited within 5 cm of the limiter radius (Fig. 3). The central ^{3}He density with and without the gas puff is shown for a high density [Fig. 7(b)] and a low density [Fig. 7(c)] case. In the high density case, the ^{3}He density rose rapidly following the gas puff and continued to rise for the duration of the neutral beam injection. In the low density case, the ^{3}He density showed a similar initial rise which peaked and then decreased steadily. These two cases are to be compared to the solutions of a cylindrical diffusion equation with constant diffusion coefficient and a delta-function initial density at a radius of 35 cm.

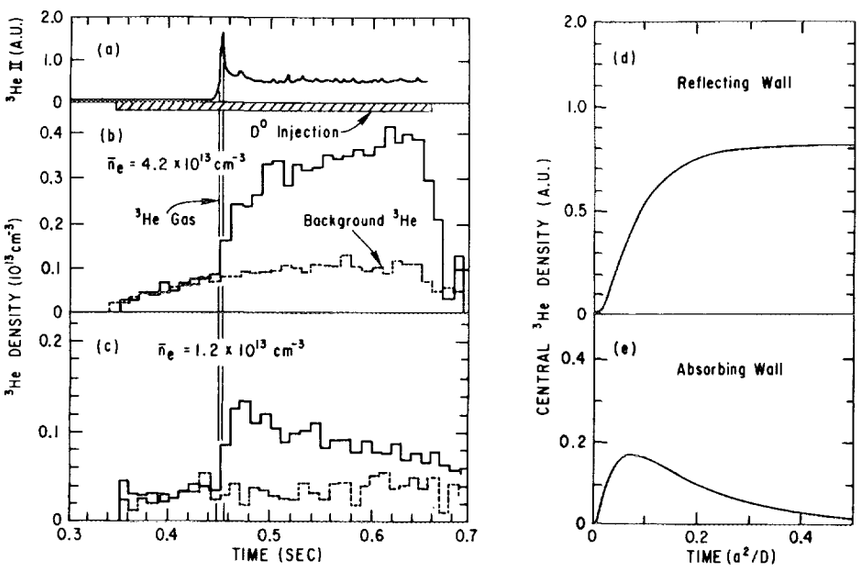

FIG. 7. Time evolution of (a) ^{3}He II spectral line intensity. (b) ^{3}He density for $\bar{n}_e = 4.2 \times 10^{13}$ cm^{-3} (with and without the ^{3}He puff). (c) ^{3}He density for $\bar{n}_e = 1.2 \times 10^{13}$ cm^{-3} (with and without the ^{3}He puff). (d) Calculated density evolution for a diffusive transport with a reflecting wall. (e) Calculated density evolution for a diffusive transport with an absorbing wall.

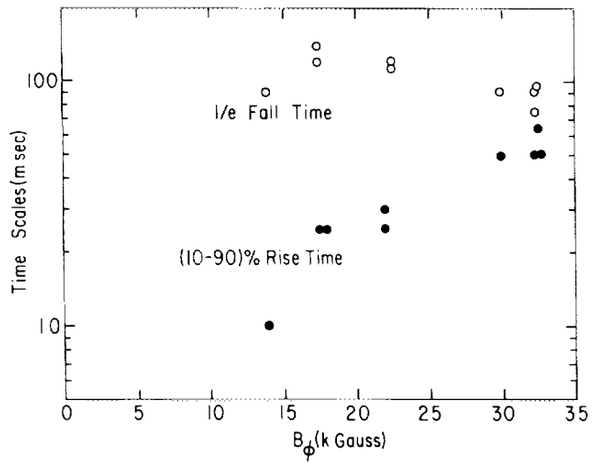

FIG. 9. ^{3}He penetration and exhaust times vs toroidal magnetic field.

The time evolution of the average ^{3}He density inside 20 cm is shown for reflecting wall [Fig. 7(d)] and absorbing wall [Fig. 7(e)] boundary conditions. The initial density rise in this model is similar for the two boundary conditions, but the long time behavior differs markedly as particles are taken out of the system by the absorbing wall.

The rise in the central ^{3}He density following a short (5 → 10 ms) ^{3}He gas puff at the plasma edge [Fig. 7(a)] indicates that the transport time of ^{3}He ions to the plasma center is (20 ± 10) ms, increasing modestly with density (Fig. 8) and toroidal magnetic field (Fig. 9). This time scale is comparable to previous spectroscopic measurements for the transit times of moderate and high Z impurity ions in PLT.[18] The inward transport time is consistent with a diffusion coefficient of $(4 \pm 2) \times 10^3$ cm^2/s or an inward directed velocity of $(2 \pm 1) \times 10^3$ cm/s, which are $\sim 10 \rightarrow 10^2$ times larger than the corresponding neoclassical particle diffusion coefficient or Ware pinch velocity.

The exhaust time for ^{3}He was long ($\geqslant 10\ \tau_{E_e}$), consistent with strong recycling and poor ^{3}He pumping at the plasma edge. However, the pumping rate is about ten times faster than for neutral ^{3}He to be removed by the PLT vacuum pumps. The helium exhaust process was stronger at low plasma density, which may have been caused by a change in the plasma edge conditions. The residual ^{3}He density left from the previous discharge was approximately 1/2 → 1/5 of the maximum ^{3}He density in that discharge (Fig. 10), indicating that considerable ^{3}He was retained in the vessel walls. Co + counter neutral beam injection caused higher residual ^{3}He densities than either Co or counter injection alone (at 1/2 of the beam power).

C. Tritium density measurements

Density measurements by nuclear diagnostics is best utilized when determining small tritium concentrations in predominantly deuterium plasmas ($n_t/n_d \approx 10^{-4} \rightarrow 10^{-1}$). The attractiveness of the tritium measurement is that since the triton and deuteron have the same Coulomb barrier, the ratio of the d–t /d–d cross sections is about constant independent of relative velocity. Thus,

$$n_t \simeq 10^{-2} n_d (I_{dt}/I_{dd}), \tag{7}$$

independent of the origin of the fusion reactions. Furthermore, since the $t(d,n)\alpha$ cross section is large, it seems likely that sensitive tritium density measurements are possible. Experimentally, the difficulty is in selectively measuring 14-MeV neutron emission levels in the range $10^{-2} \rightarrow 10$ times the 2.5-MeV neutron emission levels. Neutron spectrometers[18] and threshold detectors[17,18] are thought to be useful for such measurements. Experiments are planned on the PLT tokamak involving the laser blow-off injection of tritiated titanium in order to determine the inward tritium transport, the tritium exhaust, and the tritium removed by subsequent plasmas. Injection of 1 → 10 mCi of tritium should be detectable.

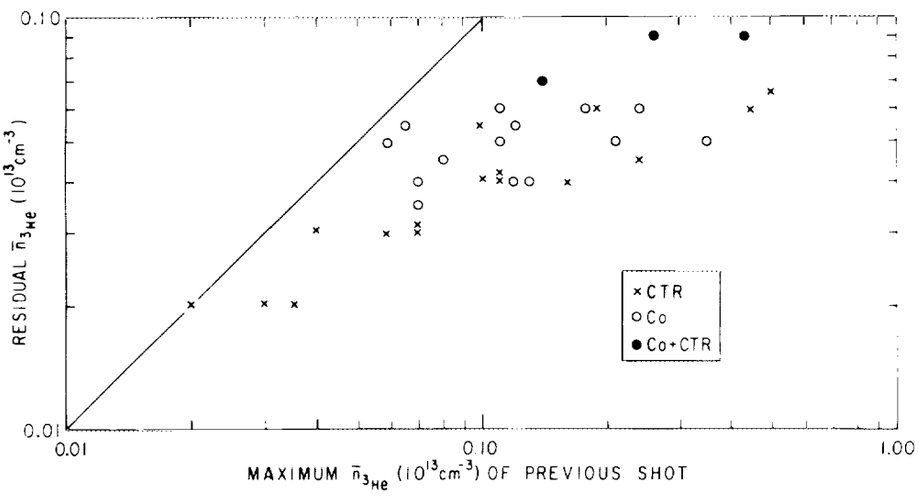

FIG. 10. Residual ^{3}He plotted vs the level of ^{3}He in the previous discharge.

[a]Present Address: Los Alamos National Laboratory, Los Alamos, New Mexico.

[1]V. V. Buzankin, V. A. Vershkov, Yu. N. Dnestrovskij, A. B. Izvozchikov, E. A. Mikhajlov, and G. V. Pereverzev, *Conf. on Plasma Phys. and Contr. Nucl. Fus. Res. Vol. I* (IAEA, Vienna, 1979), p. 287.
[2]R. J. Fonck, M. Finkenthal, R. J. Goldston, D. L. Herndon, R. A. Hulsp, R. Kaita, and D. D. Meyerhofer, Princeton University, PPPL-1908 1982.
[3]V. V. Afrosimov, Yu. S. Gordeev, A. N. Zimov'ev, and A. A. Korotov, Sov. J. Plasma Phys. **5**, 551 (1979).
[4]A. N. Zimov'ev, A. A. Korotko, E. R. Krzhizhanovskii, V. V. Afrosimov, and Yu. S. Gordeev, JETP Lett. **32**, 539 (1980).
[5]F. Engelmann and A. Nocentini, Comments Plasma Phys. Controlled Fusion **5**, 253 (1980).
[6]S. Cohen, E. Marmer, and J. Cecchi, *Proc. 7th Eur. Conf. on Cont. Fus. and Plasma Phys.* (IAEA, Lausanne, 1975), p. 137.
[7]B. M. Gokhberg, I. K. Kikoin, A. S. Knyazyatov, V. V. Mal'tsev, and G. A. Otroshchenko, Sov. Phys. JETP **18**, 295 (1964).
[8]R. L. Hickok, F. C. Jobes, and J. F. Marshall, Rev. Sci. Instrum. **37**, 591 (1966).
[9]J. D. Strachan, P. L. Colestock, S. L. Davis, D. Eames, P. C. Efthimion, H. P. Eubank, R. J. Goldston, L. R. Grisham, R. J. Hawryluk, J. C. Hosea, J. Hovey, D. L. Jassby, D. W. Johnson, A. A. Mirin, G. Schilling, R. Stooksberry, L. D. Stewart, and H. H. Towner, Nucl. Fusion **21**, 67 (1981).
[10]G. H. Miley, H. Towner, and N. Ivick, University of Illinois C00-2218-17, 1974.
[11]R. E. Chrien and J. D. Strachan, Rev. Sci. Instrum. **51**, 1638 (1980).
[12]E. B. Meservey, V. Arunasalam, C. Barnes, K. Bol, N. Bretz, S. Cohen, P. Colestock, D. Dimock, H. F. Dylla, D. Eames, P. Epthimion, H. Eubank, R. Goldston, L. Grisham, E. Hinnov, J. Hosea, J. Hovey, H. Hsvan, D. Hwang, F. Jobes, R. Kaita, G. McCracken, S. Medley, D. Mueller, N. Sauthoff, G. Schilling, J. Schivell, L. Stewart, J. Strachan, W. Stodiek, S. Suckewer, M. Ulrickson, D. Voss, S. von Goeler, G. Fankl, W. R. Wampler, and C. W. Magee, Princeton University, PPPL-1677, 1980.
[13]G. M. McCracken, S. J. Fielding, S. K. Erents, A. Pospieszczyk, and P. E. Stott, Nucl. Fusion **18**, 35 (1978).
[14]S. A. Cohen, H. F. Dylla, S. M. Rossnagel, S. T. Picraux, J. A. Borders, and C. W. Magee, J. Nucl. Mater. **76/77**, 459 (1978).
[15]R. E. Chrien, H. P. Eubank, D. M. Meade, and J. D. Strachan, Nucl. Fusion **21**, 1661 (1981).
[16]R. E. Chrien, P. L. Colestock, H. P. Eubank, J. C. Hosea, D. Q. Hwang, J. D. Strachan, and H. R. Thompson, Jr, Phys. Rev. Lett. **46**, 535 (1981).
[17]W. Heidbrink, R. Chrien, and J. D. Strachan, PPPL-1937 (1982).
[18]P. Colestock, J. D. Strachan, M. Ulrickson, and R. Chrien Phys. Rev. Lett. **43**, 768 (1979).